

A QPE Product with Blended Gage Observations and High-Resolution WRF Ensemble Model Output: Comparison with Analyses and Verification during the HMT-ARB

Edward I. Tollerud^{1,*}, John A. McGinley¹, Steven L. Mullen², Tomislava Vukicevic³, Huiling Yuan³,
Chungu Lu⁴, and Isidora Jankov⁴

¹*NOAA Earth System Research Laboratory (ESRL), Global Systems Division Boulder, Colorado USA*

²*Department of Atmospheric Sciences, University of Arizona, Tucson, Arizona USA*

³*Cooperative Institute for Research in Environmental Sciences (CIRES), University of Colorado at Boulder, and Earth System Research Laboratory (ESRL), Global Systems Division, Boulder, Colorado*

⁴*Cooperative Institute for Research in the Atmosphere, Colorado State University, Fort Collins, Colorado USA, and Earth System Research Laboratory (ESRL), Global Systems Division, Boulder, Colorado USA*

1. Introduction

Particularly in regions of extreme terrain, timely quantitative precipitation estimates (QPE) during heavy rainfall/snowfall events are critical but difficult to obtain given instrumentation density and quality issues. For these situations, it is possible that a blend of short-term forecasts with observations might perform better than purely observational estimates. In this paper, we describe an example of this kind of system, one which applies variationally-driven ensemble methods to blend WRF forecasts with gage measurements. These methods have been successfully employed in attempts to assimilate other quantities, but their application to precipitation has not been fully realized. We apply them to a case of very heavy precipitation in the Northern California Sierra Nevada Mountains during December and January of 2005-6.

2. Background and Methodology

The basic formulation of optimal data assimilation techniques assumes that information about the state of the weather can be given by quantities contained in the NWP model forecast and in observations. In inverse problem theory the information from a model and observations is combined by a conjunction of the Gaussian probability density functions (pdf's) resulting in

a new, joint posterior pdf. This conjunction can be expressed as

$$(1) \quad p_{\text{posterior}} \sim \exp(-J(x_a, y))$$

where x_a and y are modeled and measured stochastic Gaussian quantities, respectively, and J is the well known cost function (Kalnay, 2004), which we define as

$$(2) \quad J(x_a, y) = \sum_i \frac{1}{2} [(h_i(x_a) - y_i)^T R^{-1} (h_i(x_a) - y_i)] + \frac{1}{2} (x_a - x_b)^T P_f^{-1} (x_a - x_b)$$

In this initial work we have assumed that $\log x$ is normally distributed. Thus in our application, x_a is the analysis state vector containing the log of all precipitation estimates on the analysis grid, y_i is the log of observation of type i , and $h_i(x_a)$ is the transformation from the analysis state space into observation space, or “observational network operator”. $R_{y_i}^{-1}$ is the inverse covariance matrix of logged observational errors for each observation type, x_b is the log of the background precipitation vector of the same length (would be some deterministic estimate of precipitation from a model) as the analysis precipitation vector, and P_f^{-1} is the inverse covariance matrix of the logged background precipitation errors derived from the 3-km ensemble. This matrix is the focus

*Presenting Author: Edward.tollerud@noaa.gov
303-497-6127

of our ensemble post processing; for a limited domain P_f may be fully recoverable.

When the observational operators h_i are linear and are combined into one operator they are conveniently denoted as H . The posterior solution in this case is expressed respectively in terms of mean and covariance as:

$$(3) \quad \begin{aligned} x_a &= x_b + \left(HP_f H^T + R\right)^{-1} H^T R^{-1} (y - Hx_b) \\ P_a &= \left(H^T R^{-1} H + P_f^{-1}\right)^{-1} \end{aligned}$$

Background error covariances are determined using a hybrid scheme that involves a linear combination of both time-dependent (climatological) and time-independent (ensemble forecast-based) covariances. The relative influence of the two are determined via the settable coefficient α in the equation

$$(4) \quad P_f = \alpha P_c + (1-\alpha) P_e$$

where P_c is the climatological covariance from many cases, described below and α is a weight that goes from 0 to 1. P_e is the ensemble derived covariance. Climatological covariances are determined from a set of 95 cases (actually 6h time periods) during the IOPs for the first two HMT-ARB field exercises in 2005-6 and 2006-7.

For model forecast input, we have used a set of time-lagged multi-model ensembles for NOAA-HMT forecast applications (Yuan *et al.* 2008a). The time-lagged ensemble members in these runs are generated from a set of WRF-based forecasts initialized every 6-hours using NOAA-LAPS (Albers *et al.* 1996), and evaluated at the same forecast projection time. Only the closest 3 lagged ensembles are used in order to avoid large error contamination due to longer model integrations. Because this limited ensemble size can cause serious rank-deficiency problems in the retrieved background error covariance matrix, a combination of time-lagged ensembles with a set of mixed physics ensembles are used to increase the ensemble size (Yuan *et al.* 2008b). The mixed physics ensemble consisted of simulations performed by using Weather Research and Forecasting (WRF) numerical model with both Advanced Research and Forecasting (ARW) and Non-hydrostatic Mesoscale Model (NMM) dynamical cores. The following microphysical schemes were used: Ferrier *et al.* (2002), Thompson *et al.* (2004) and Schultz (1995).

As observational input to our data assimilation technique, we use 6h accumulated precipitation at operational hourly gages available from the Hydrometeorological Automated Data System (HADS) managed by the Office of Hydrology of the National Weather Service. These data are first screened by a set of automated daily quality control procedures. To establish an independent sets of gages for verification purposes, we designate a set of verification gages for each of several separate analysis runs by withholding a small number (3-5) of gages from each run. An example for a single 6-h period is shown on Fig. 1. This procedure resulted in 183 verification pairs from the five initial runs and the eight time periods. Tests showed that the resulting QPE fields were not greatly impacted by the small number of withheld gages.

3. Results from IOP 4

Two of the five runs with withheld gages are shown in Fig. 1, which compare a single time period QPE with a gage-only analysis using STMAS (Xie *et al.* 2005). There is general similarity between these two runs in both the STMAS and QPE sets, a similarity that extends to the other three runs. A significant difference in smoothness and detail is also clearly seen between STMAS and the optimal QPE, which at this time has a striking east-west pattern. We propose that the difference in detail is a result of the good resolution of the model fields (unavailable to the STMAS analyses), the physics packages that can help build accurate precipitation fields, and the presence of high-resolution terrain. Another difference between the two estimates is that the STMAS analyses seem to retain larger values over the eastern domain boundary (the region including Lake Tahoe) than the optimal QPE.

While Fig. 1 displays a time period for which the optimal analysis performs well (at least qualitatively), other time periods and computational parameters can give worse results. For instance, a QPE plot during an earlier 6h period of IOP 4 when light general rain was falling over the domain (Fig. 2) exhibits large and apparently spurious precipitation maxima. Part of the problem in this case is likely traceable to a poor forecast; the ensemble mean is late getting the precipitation started, with the result that predicted rainfall is too small over most of the domain. This poor forecast in turn produces

inaccurate error covariances and a poor optimal QPE field. Other factors may also be present, including the proper determination of weights for the climatological error covariances that are applied in the computations that lead to the QPE analyses, and the best selection of lag times. We will discuss these possibilities in more detail in the conclusions. Although our preliminary sensitivity tests have not shown this to be

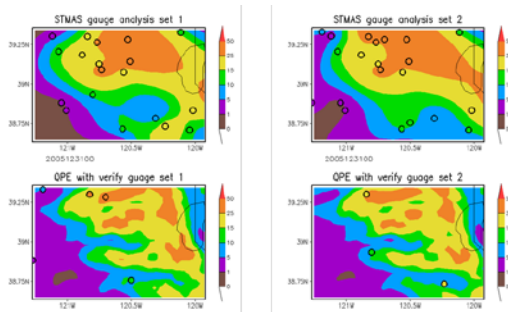


FIG. 1. Gage-only (STMAS; top row) analyses and optimal QPE (bottom row) for two sets of analyses of 6h precipitation ending at 0000 UTC 12 December 2005 in the ARB domain. Top row show locations of gages used in the analyses; bottom row displays gages withheld from analyses for later use in verification. Legends are in mm.

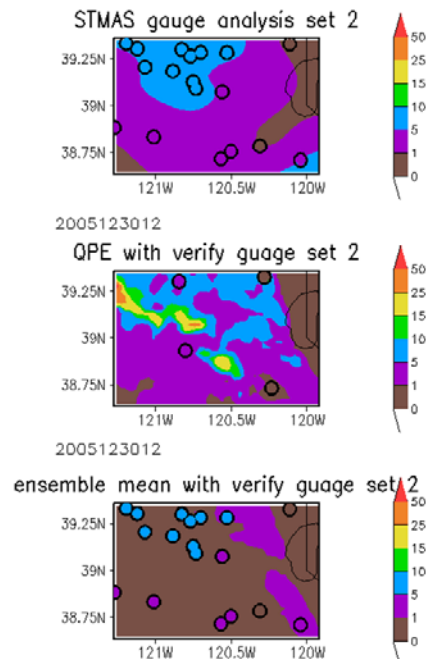


FIG. 2. STMAS and optimal QPE analyses (top and middle), and WRF ensemble mean forecast (bottom) for 6h precipitation ending at 1200 UTC 30 December 2005. Legends are in mm. Analyses gages are shown for the STMAS analysis and WRF forecast, and withheld gages are shown for the optimal QPE analysis.

universally true, it does appear that the optimal QPE computations encounter greater difficulty for scenarios with lighter and more general rainfall.

With five sets of analyses during eight 6h periods, and 3-5 withheld gages for each, it is possible to compute quantitative statistics and verification scores with 183 verification gage precipitation observations matched with STMAS, optimal QPE, or ensemble forecast grid points. The scatter plot of Fig. 3 provides a general overview of the observation pairs that will make up these score computations. The forecast ensemble mean rainfall points show a strong tendency to appear above the one-to-one line of the verification observations, an indication of over-prediction. Both the STMAS and optimal QPE points generally straddle the line (that is, show less sign of overall bias), with the QPE points showing less scatter about that line than those for the STMAS analyses. There are a few QPE outliers that may account for some reduction in the correlation values; see for instance the QPE point with 50 mm precipitation that matches to a gage value of less than 10 mm. Overall, the ensemble forecast precipitation and the optimal QPE have correlation coefficients that are roughly equal, while the STMAS correlation is well below that of the other two.

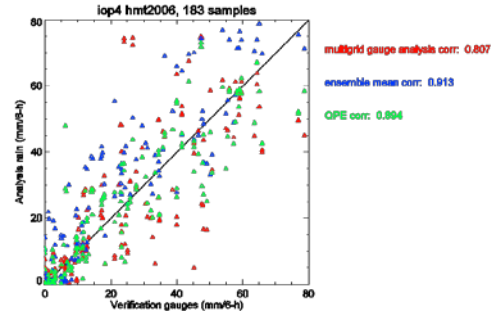


FIG. 3. Verification gage observations (horizontal axis, mm) plotted against nearest grid point values of STMAS gage-only analyses (red), 12-member ensemble mean WRF forecasts (blue) and optimal QPE analyses (green) for 8 6h periods during IOP 4 (horizontal axis, mm). Spatial correlation values are also shown.

The IOP 4 domain-averaged precipitation rates and error estimates of Fig. 4 reveal, first, that optimal QPE and STMAS are indeed not biased as compare to overall verification gage averages. WRF forecasts, on the other hand, show a full 6 mm large bias over this IOP. While the mean absolute error between the ensemble mean and gages, and between STMAS and

gages, is about the same, for QPE it is significantly less. Similarly, the root mean square error for QPE is also well below that of STMAS or WRF forecasts. This improved performance for optimal QPE is reflected also in the equitable threat scores (ETS) of Fig. 5. For the range of thresholds most meaningful for this heavy rain event, (between 0.25 and 1.5 in), the QPE ETS is larger than (or in one case equivalent to) the other two, and occasionally is a full point better either of them.

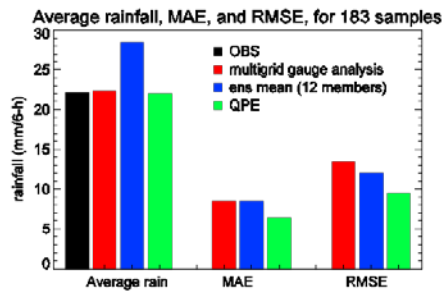


FIG. 4. HMT-ARB domain-average 6h rainfall (left bar cluster), mean absolute error (middle) and root-mean-square error (right) for all verification pairs during IOP 4. The black bar indicates straight average including all gages in the domain; other colors are as indicated in the legend.

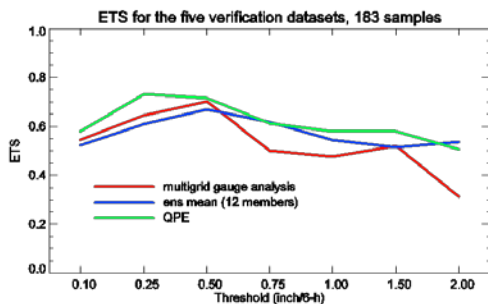


FIG. 5. Equitable threat scores (ETS) computed at verifying gage locations for the analyses and forecasts indicated.

4. Conclusions and Further Research

In general, this case study demonstrates that combining high-resolution ensemble forecasts with gage data using an optimal estimation methodology can successfully produce high-resolution QPE over a mountainous river basin that is superior to gage-only analyses (as measured by quantitative verification scores using withheld gages). However, it appears that occasionally bad error covariances from poor ensemble forecasts or other causes can result in

spurious extreme rainfall in the QPE fields. These results suggest that further investigation of the forecast skill of ensemble forecasts is needed. Other important subjects for future research involve the specification of computational parameters in the optimal analysis methodology. For instance, sensitivity studies already performed demonstrate that when error covariances derived from scenario-specific model climatology are strongly weighted, the root mean square errors of the QPE fields are smaller (Fig. 12). The figure also shows that for low weightings, there is a dramatic dependence on the length of forecasts (i.e., number of lags). On the other hand, the QPE analysis is less sensitive to the inclusion of more time-lagged members when the model climatology weights are larger. More sensitivity tests of this kind are required before the best combination of parameters can be specified. Another important test should be the determination of the impact of our Gaussian assumption for the logarithm of precipitation amount. Subsequent analyses suggest that a cubed root representation would be more appropriate.

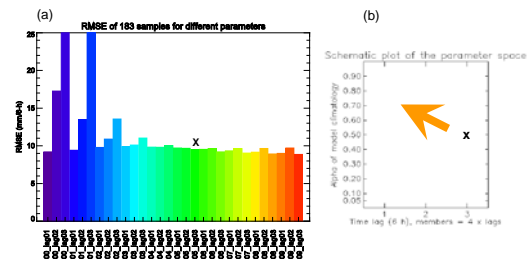


FIG. 6. (a): Root-mean-square errors (RMSE) during IOP 4 for different combinations of model time lag ensemble members (1-3 6h periods) and climatological error covariance weightings (0.1 to 0.9; coefficient alpha in Section 3). (b): Idealized schematic parameter space diagram for model time lags and model climatology weighting. The 'X' symbols on both panels indicate the set of parameters used in verification computations and analyses in previous figures; the arrow in panel (b) indicates the direction in parameter space required to move toward improved analyses.

Other future plans include extension of this research to other IOPs during the HMT project and to a larger region including more river basins in the 3km model domain to capture a larger sample set of observations. Both verification scores and the spectral analysis results can be better confirmed by this improved sampling. Other data sources such as radar observations during the HMT project can be added to the QPE

analysis. Possibly the inclusion of radar data can help confirm the validity of the small-scale ridge-valley circulations implied by the ensemble forecasts and the precipitation estimates, as well as by the spectral analyses. The QPE scheme will be examined for different ensemble configurations, such as combinations of various physics options and multiple models. With the present results in mind, a further question that can be addressed is this: If we assume a given QPE field is truth, is it possible to design a rain gage network that optimizes basin averages and narrows the analysis PDF in meaningful ways?

Acknowledgments

We thank Steve Koch, GSD director, for funding for this project through the Director's Discretionary Research funds. We also thank Annie Reiser for her technical review.

References

- Albers, S., J. A. McGinley, D. Birkenheuer, and J. Smart, 1996: The Local Analysis and Prediction System (LAPS): Analyses of clouds, precipitation, and temperature. *Wea. Forecasting*, **11**, 273-287.
- Ferrier, B. S., Y. Jin, Y. Lin, T. Black, E. Rogers, and G. DiMego, 2002: Implementation of a new grid-scale cloud and rainfall scheme in the NCEP Eta model. Preprints, *15th Conf. On Numerical Weather Prediction*, San Antonio, TX, Amer. Meteor. Soc., 280-283.
- Hong, S.-Y., J. Dudhia, and S.-H. Chen, 2004: A revised approach to ice microphysical processes for the bulk parameterization of clouds and precipitation. *Mon. Wea. Rev.*, **132**, 103-120.
- Kalnay E., 2004: *Atmospheric Modeling, Data Assimilation and Predictability*. Cambridge University Press, 341 pp.
- Lu, C., H. Yuan, B. Schwartz, and S. Benjamin, 2007: Short-range forecast using time-lagged ensembles. *Wea. Forecasting*, **22**, 580-595.
- Noh, Y., W.-G. Cheon, S.-Y. Hong, and S. Raasch, 2003: Improvement of the K-profile model for the planetary boundary layer based on large eddy simulation data. *Bound.-Layer Meteor.*, **107**, 401-427.
- Schultz, P. J., 1995: An explicit cloud parameterization for optional numerical weather prediction. *Mon. Wea. Rev.*, **123**, 3331-3343.
- Thompson, G., R. M. Rasmussen, and K. Manning, 2004: Explicit forecasts of winter precipitation using an improved bulk microphysics scheme. *Mon. Wea. Rev.*, **132**, 519-542.
- Troen, I., and L. Mahrt, 1986: A simple model of the atmospheric boundary layer: Sensitivity to surface evaporation. *Bound.-Layer Meteor.*, **47**, 129-148.
- Xie, Y., S.E. Koch, J.A. McGinley, S. Albers, and N. Wang, 2005: A sequential variational analysis approach for mesoscale data assimilation. *21st Conf. on Weather Analysis and Forecasting*, Washington, D.C., Amer. Meteor. Soc., CD-ROM, 15B.7.
- Yuan, H., J. A. McGinley, P. Schultz, C. Anderson, and C. Lu, 2008a: Evaluation and calibration of short-range PQPFs from time-phased and multimodel ensembles during the HMT-West-2006 campaign. *J. Hydrometeor.*, **9**, 477-491.
- Yuan, H., C. Lu, J. McGinley, P. Schultz, L. Wharton, and B. Jamison, 2008b: Short-range quantitative precipitation forecast (QPF) and probabilistic QPF using time-phased multi-model ensembles. In review, *Wea. Forecasting*.